16th World Conference on Earthquake, 16WCEE 2017

Santiago Chile, January 9th to 13th 2017

Paper N° 3875

Registration Code: S-T1462305856

SENSITIVITY ANALYSIS OF SEISMIC PERFORMANCE OF DRY CASK STRUCTURES

M. Ebad Sichani[(1)], J. E. Padgett[(2)]

[(1)] *Graduate Research Assistant, Department of Civil and Environmental Engineering, Rice University, me15@rice.edu*
[(2)] *Associate Professor, Department of Civil and Environmental Engineering, Rice University, Jamie.padgett@rice.edu*

Abstract

This paper analyzes the probabilistic seismic performance of dry cask structures with a focus on the sliding response. Dry casks are reinforced concrete cylindrical tanks that are used for the purpose of interim storage of spent nuclear fuel in the United States. These structures are typically located at independent spent fuel storage installations of nuclear facilities, with a higher concentration on the eastern coast. The storage tanks are freestanding structures that are prone to sliding and rocking during strong earthquakes, which might lead to impact between adjacent casks. Catastrophic consequences of damage to these structures make it necessary to study their seismic performance. To perform the seismic analysis, twelve parameters that might affect the seismic response were selected based on the literature. Latin hypercube sampling was employed to generate 160 configurations with different geometric, material, and structural properties. Finite element models of the problem were developed to determine the response of these structures under three-component ground motions. Sliding of the cask relative to its supporting pad was calculated, and probabilistic demand models were developed for the maximum sliding distance. The resulting parameterized models can support risk assessment of a broad range of reinforced concrete dry cask storage systems located in seismic zones. Furthermore, sensitivity analysis was performed to determine the parameters which have a significant influence on the seismic response of these structures. The sensitivity analysis can help designers have a better understanding of the effect of changing different parameters on the seismic response and fragility of this storage system.

Keywords: concrete dry cask; seismic performance; probabilistic demand model

1. Introduction

Safe and efficient storage of spent nuclear fuel has been an important issue in the management of nuclear power plants. Long-term storage of the nuclear waste, such that it facilitates decaying of the spent fuel's radioactivity, is often deemed the best option. However, it is very difficult to select a suitable site that satisfies all safety requirements [1]. The storage process of the spent fuel includes: (1) short-term storage in which the spent fuel is stored in spent fuel pools; (2) interim storage in which the nuclear waste is transferred to independent spent fuel storage installations (ISFSI) of nuclear power plants and stored in special structures called dry casks; (3) long-term storage [1]. As many spent fuel pools in nuclear power plants are reaching their full storage capacity, many utilities have been transferring their old spent fuels to dry casks in their ISFSI in order to be able to continue their regular operations [2]. These dry casks are reinforced concrete cylindrical tanks which are used for the interim storage of the nuclear waste. Typically, a steel canister that contains the nuclear waste is transferred from the plant to the location of the casks and placed inside the cask. Since dry casks are freestanding structures, there are concerns about their stability subject to natural and man-made hazards. Although the canister and concrete walls of the casks should be designed such that they can continue their functions to prevent any radiation from the spent fuel in case of tip-over or impact between adjacent casks, the risk of failure of these structures should still be assessed due to severe consequences that any released radiation might have on human health and the environment.

Ground motions are one of the natural hazards that might cause the instability of dry casks and should be included in the risk analysis of ISFSI projects [2]. In this regards, several studies have been conducted on the seismic performance of dry cask structures. Moore et al. [3] and Bjorkman et al. [4] used a finite element method to analyze the effects of pad flexibility, soil properties, and cask layouts on the seismic response of HI-STORM 100 casks, a commonly used type of dry casks. Singh et al. [5] presented a deterministic dynamic analysis method based on Lagrange's equation of motion to predict the seismic response of dry casks. They suggested that the maximum sliding of a cask should be less than ¼ of the cask's diameter. Shaukat and Luk [6] used sophisticated 3D finite element models to address the dynamic coupling of cask, pad, and underlying soil foundation. They investigated the effect of cask design, soil properties, friction coefficient, and earthquake records on the seismic response of dry casks and showed that the casks might slide in strong earthquakes, but the maximum angle of rotation is negligible for different cask designs. In a similar study, Luk et al. [7] analyzed dry casks with two different layouts under different ground motion time histories adjusted to three spectral shapes. Although they considered other parameters in the study, such as various coefficients of friction and soil materials, they did not elaborate on the results and just concluded that earthquake time history is an important parameter which governs the cask's behavior. Ko et al. [1] used 3D explicit finite element method to analyze the seismic response of a dry storage facility, planned to be installed in Taiwan, and showed that the cask slides but does not tip over subject to design earthquakes.

None of the mentioned studies take a probabilistic approach in dealing with the seismic response of dry casks, or characterizing uncertainty in the response as a function of random variables. However, seismic risk assessment of these structures requires estimating the probability of failure of the casks subject to seismic loads. In this regards, the U.S. Nuclear Regulatory Commission provides guidance for the parametric evaluation of the seismic behavior of dry casks in NUREG/CR-6865 [8] without considering the uncertainties in the problem. NUREG-1864 [2] conducts a probabilistic risk assessment and estimates the annual risk to the public from different man-made and natural hazards. However, since the study does not perform uncertainty analysis and just uses simplified models, the provided results might change in case uncertainty is considered. This paper develops probabilistic seismic demand models for the sliding response of the reinforced concrete dry cask structures, considering a range of epistemic and aleatory uncertainties inherent in the problem such as the uncertainties in the material and geometric properties and applied seismic loads. The developed probabilistic models are quite useful in risk analysis of this storage system because of their application in rapidly estimating the probability of failure of the casks under strong ground motions without the need for additional 3D nonlinear finite element models, which are expensive and time-consuming.

2. Seismic demands on concrete dry casks

2.1 Finite element modeling

Developing probabilistic demand models requires virtual experimental data. This data was generated using nonlinear finite element models of the problem, which were analyzed by the explicit solver of LS-DYNA [9]. In order to verify the developed finite element models, results from an experimental study conducted by Shirai et al. [10] were used. The tested model by Shirai et al. was a scaled cask with the height of 1.9 m and diameter of 1.23 m, which was subjected to the major horizontal and vertical components of JMA Kobe 1995 ground motion. A finite element model with the same dimensions, material models, and ground motion time histories was developed for verification purposes. Half of the cask was considered in this model because of the symmetric geometry and the loads in the experimental test. Fig. 1 shows the comparison between the results of the experimental test and the results provided by finite element modeling. This comparison reveals that the response obtained from the finite element model has a very good agreement with the experimental test results. Although the set of comparative analyses is limited by available data, the quality of comparisons shown offers confidence in the model. Hence a similar finite element modeling strategy is adopted when conducting simulations for development of probabilistic seismic demand models.

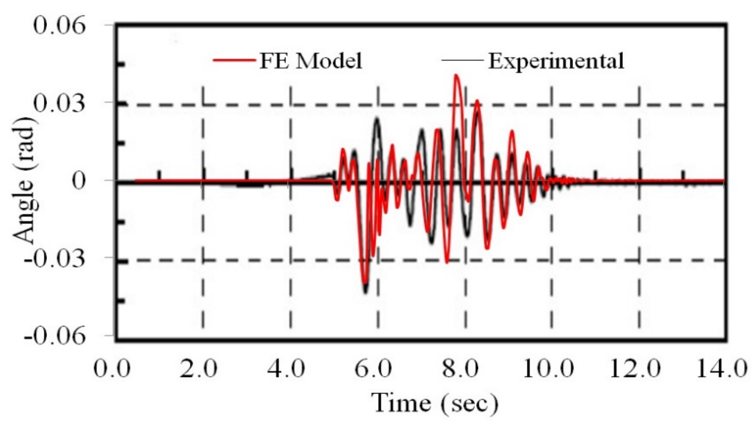

Fig. 1 – Comparison between the results obtained from the study conducted by Shirai et al. [10] and the results obtained from the corresponding finite element model developed in this study

There were slight differences in the finite element models used in this study to generate the virtual experimental data than the model developed for verification purposes. That is, these models considered full geometry of the problem and used all three components of ground motions. In addition, the soil below the pad was modeled by linear spring and dashpot elements. It should be mentioned that the nonlinear contact between the cask and the pad was common in both cases, and the comparison presented by Fig. 1 showed that the contact model, which is the only nonlinear part of the model, worked well in the developed finite element model. Fig. 2 shows a sample of the finite element models used in this study, in which the cask, canister, and pad were modeled by solid elements. Since the focus of the study was the seismic response of the cask, and the modeled parts were not expected to behave nonlinearly during basic sliding response under ground excitation, a linear elastic model was used for the material behavior of all the parts. The soil was modeled by vertical and horizontal springs and dashpots, whose stiffness and damping coefficients were determined based on FEMA 356 Prestandard [11] formulas, which are also available in NIST GCR 12-917-21 [12]. Although some studies, like the one performed by Ko et al. [1], model the soil body by 3D solid elements, this study adopted distributed discrete elements to help reduce the computational complexity because of the large number of simulations required to develop probabilistic demand models. The nonlinear contact between the cask and the pad was simulated by AUTOMATIC-SURFACE-TO-SURFACE model, which is recommended for models in which the orientation of parts relative to each other cannot always be predicted as the analysis goes ahead [9]. This contact model is a two-way search algorithm in which the contact forces are evaluated by the penalty approach [9]. Three-component ground motions were applied to the soil elements' end nodes, and the cask's maximum sliding was determined by post-processing the analysis time history results. The cask's sliding vector in each time step was calculated by subtracting the horizontal displacement of the cask's bottom surface from the pad's horizontal displacement. The magnitude of the resultant vector was considered as the cask's (relative) sliding whose maximum value was used to develop the probabilistic demand models. Such probabilistic demand models predict the uncertain peak sliding of the cask given input cask and earthquake parameters, thus averting the need for additional numerical simulations.

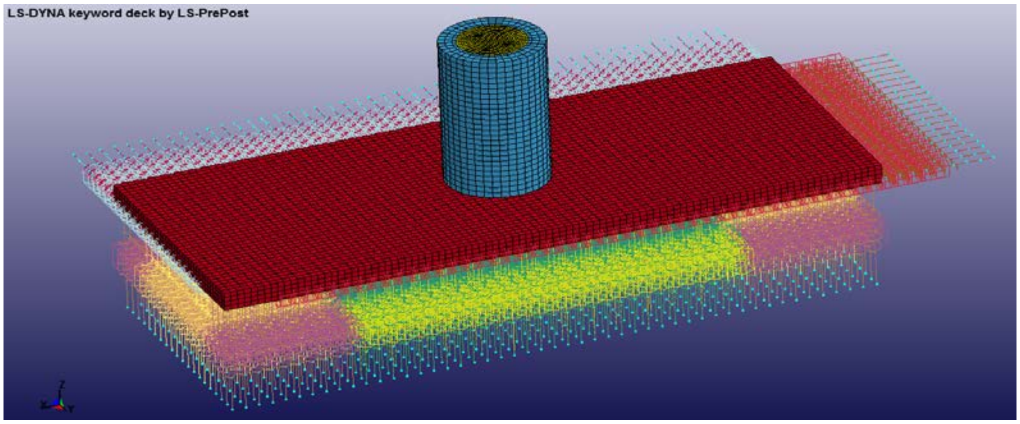

Fig. 2 – Sample finite element model used to generate virtual experimental data

2.2 Experimental design

Running nonlinear finite element models should provide a large amount of information and, at the same time, should consume acceptable computational resources. To accomplish these goals, an experimental design procedure was used in this study to maximize the information content and minimize the associated computational costs. Based on the literature, the geometric, material, and structural parameters that might impact the seismic response of the dry casks were chosen, and the ranges of these parameters were determined. The Latin hypercube sampling technique [13] was used to generate 160 structural configurations for the dry casks. This technique is a space filling technique which maximizes the minimum distance between the data points. The considered ranges, which are shown in Table 1, are broad enough to cover realistic cask configurations produced by different manufacturers. Therefore, the probabilistic demand models developed in this study are general and appropriate to be used for estimating the seismic response of different types of casks.

2.3 Ground motion selection

To take into account earthquake characteristics of different regions in the United States, the country was divided into three regions: west, central, and east. A ground motion selection method, proposed by Baker et al. [14], was employed, in which earthquakes are selected whose response spectra match a target response spectrum for the region. The target response spectra were determined by using the USGS (United States Geological Survey) hazard curve application, which is available at *http://geohazards.usgs.gov/hazardtool/application.php*. This application takes geographical coordinates of the desired location as input and outputs hazard curves and uniform hazard response spectra (UHRS) for different hazard levels. In this study, an initial set of UHRS with different shapes was selected for each region for the hazard level of 2% probability of exceedence in 50 years. The UHRS selection took into account the locations of existing dry casks, locations with appreciable seismic hazards, and different soil types in each location. Eight spectra, out of the inital set of response spectra, were selected as the final target response spectra to be used in the ground motion selection process for each region. The final spectra were chosen so that they reflected different spectral shapes and different intensities. Ten ground motions were selected for each of the target response spectra, which resulted in 80 earthquake records selected for each region, which means 240 ground motions were selected as the output of the ground motion selection procedure. This ground motion selection process produced earthquake records with different frequency contents and intensity measure ranges, while still respecting the seismic hazard characteristics of each region. NUREG-0800 [15] requires that nuclear power plants be analyzed subject to earthquakes with horizontal PGAs (Peak Ground Accelerations) larger than 0.1 g. As a result, some of the records from the original ground motion selection were scaled. In addition, to produce a broader range of earthquake intensity measures and significant seismic responses for probabilistic seismic demand modeling, additional earthquakes were scaled (with an average scale factor of 2.03) so that half of the final suite of ground motions were scaled. For the three regions (west, central, and east), each selected earthquake was randomly assigned to two of the developed finite element models. As a result, 480 different models were generated, which were analyzed using the explicit solver of LS-DYNA, and the analysis results were used to develop probabilistic seismic demand models for the sliding response.

Table 1 – Geometric, material, and structural parameters and the associated ranges used in experimental design

Variable	**Symbol**	**Unit**	**Range**
Cask wall thickness	t_C	m	0.5 – 0.8
Cask height	H_C	m	5.5 – 6.0
Cask outer diameter	D_C	m	3.2 – 4.0
Cask weight	W_C	ton	120 – 180
Height of the cask's center of gravity over the cask's total height	α_G	---	0.48 – 0.52
Cask concrete compressive strength	f'_{cc}	MPa	20 – 55
Pad thickness	t_P	m	0.5 – 1.2
Pad length	L_P	m	9 – 60
Pad concrete compressive strength	f'_{cp}	MPa	20 – 55
Cask-pad friction coefficient	μ	---	0.2 – 0.8
Soil shear wave velocity	C_S	m/s	150 – 2000
Damping ratio	ξ	---	0 – 0.1

3. Development of probabilistic demand model for sliding response

3.1 Static analysis of the problem

This section performs static analysis on the sliding response of the dry cask in order to gain some insight into the physics of the problem and to detect the most important parameters. Consider the dry cask as a 2D rigid body as shown in Fig. 3. The mass of the body is m, its outer diameter is D_C, and the coefficient of friction between the cask and the pad is μ. To simplify the problem, the static and dynamic coefficients of friction are assumed to be equal. The horizontal and vertical accelerations at the center of gravity (CG) of the cask are a_H and a_V, respectively. Therefore, the inertial forces applied to the cask are ma_H and ma_V. To consider the worst case, the vertical inertial force is assumed to be upward. Other forces applied to the body are the weight, mg, the normal force applied by the support, N, and the friction force, μN.

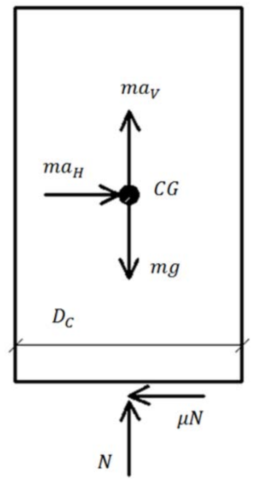

Fig. 3 – Free body diagram used for a simplified static analysis of the sliding response of the cask

Equilibrium in the horizontal direction at the onset of sliding results in the following equations:

$$ma_H = \mu N \tag{1}$$

The normal force is given by Eq. (2):

$$N = mg - ma_V \tag{2}$$

Therefore

$$ma_H = \mu(mg - ma_V) \tag{3}$$

This results in the following classification:

$$\begin{cases} ma_H < \mu m(g - a_V) \Rightarrow \text{Cask does not slide} \\ ma_H > \mu m(g - a_V) \Rightarrow \text{Cask slides} \end{cases} \tag{4}$$

Simplifying m from both sides, rearranging, and introducing a new parameter as $R_S = \frac{\mu}{\frac{a_H}{g-a_V}}$, Eq. (4) results in:

$$\begin{cases} R_S > 1 \Rightarrow \text{Cask does not slide} \\ R_S < 1 \Rightarrow \text{Cask slides} \end{cases} \tag{5}$$

Eq. (5) shows that sliding response is related to R_S. That is, for large values of this parameter, the cask's sliding is negligible, and for small values of R_S, the cask is very vulnerable to sliding. In other words, we expect the cask's sliding to decrease as R_S increases.

The static analysis showed that the sliding response is related to the coefficient of friction between the cask and the pad, the accelerations at the cask's center of gravity, and the introduced parameter, R_S. Although R_S is defined by μ, a_H, and a_V, the relation between the actual sliding response under dynamic loads such as earthquake excitation and these parameters (μ, a_H, and a_V) may differ from the form of R_S. The effect of these parameters along with other parameters on the seismically induced sliding response was tested through probabilistic seismic demand modeling and will be explained in section 3.2.

3.2 Probabilistic seismic demand model for the sliding response

A probabilistic seismic demand model (PSDM) offers a relationship between the influential parameters in a problem and the response. The PSDM takes the model parameters, which can be random variables, as inputs and predicts the target response (e.g. maximum sliding of a cask). To develop the probabilistic demand models in this study, the target response (e.g. maximum sliding of the casks) was determined from the finite element analysis outputs, and stepwise regression was used in MATLAB along with transformations applied to the predictors and response. A constant term is the only building block in the first step while using stepwise regression for model development [16-18]. In the next steps, one term is added to the model each time, and the efficiency of the added term is determined based on a selected criterion. If the added term improves the model efficiency, it is kept; otherwise, it is removed [16-18]. The added term could be a single predictor or a combination of predictors based on the degree of the polynomial being fitted. In this study, the largest polynomial degree tested was 3, and "deviance" [16-18] was the decision-making criterion. The final PSDM was developed using the best set of predictors provided by the stepwise regression. The accuracy of the developed models was determined by the 5-fold cross validation (CV) method [19]. This method divides the input data into five subsets, called folds, finds the best model using four folds, and tests the accuracy of the resulting model on the fold which was not included in the training data. This process is repeated five times, and the average R^2 of all the trials is reported as the result. The cross validation method validates the performance of the model in predicting the target response. In order to include the best predictors in the model, those with p-values lower than 0.05 were kept in the final PSDM [16-18]. Logarithmic transformations, applied to predictors and response, were adopted since they improved the accuracy of the probabilistic seismic demand models. In addition, a simple linear combination of the predictors was used in the final PSDMs because of the simplicity and accuracy provided by this form.

The static analysis, explained in section 3.1, showed that the accelerations at the cask's CG are important parameters in predicting the sliding response. Because of the importance of these parameters, PSDMs capable of predicting the maximum horizontal and vertical accelerations of the cask's CG ($a_{CG,H}$ and $a_{CG,V}$, respectively) were developed in the first step. To develop these models, it was necessary to estimate the motion on top of the pad, which eventually causes the cask motions. In order to estimate the pad's motion, the pad was assumed to be a single degree of freedom (SDOF) system whose mass was the summation of the pad mass and the cask mass, and its stiffness was provided by the soil. As explained in section 2.1, the soil was modeled by spring and dashpot elements in three directions. Therefore, adding the stiffness of all the springs in one direction would result in the equivalent stiffness for the SDOF system in that direction. This approach resulted in an estimation for the natural periods of the pad-soil system in three directions. The estimated natural periods happened to be very small, which means the maximum acceleration of the pad in each direction should be close to the PGA of the corresponding earthquake component. Therefore, the PGAs of the ground motion were used as the earthquake intensity measures (IMs) in this study. The validity of adopting these IMs was also examined when testing the goodness of fit measures of the PSDMs (showing that using these IMs as predictors resulted in high quality predictive models). The ground motion PGAs along with coefficient of friction and the geometric, material, and structural properties of the cask were tested as the predictors to develop probabilistic demand models for the maximum horizontal and vertical accelerations at the cask's CG. Through the process explained in this section, the models shown in Eq. (6) and Eq. (7) resulted for $a_{CG,H}$ and $a_{CG,V}$.

$$\log a_{CG,H} = 0.21\mu - 0.051PGA_H + 1.024\log PGA_H \tag{6}$$

$$\log a_{CG,V} = 0.288 + 0.334\mu + 0.852\log PGA_H - 0.249PGA_V + 0.855\log PGA_V \tag{7}$$

$$PGA_H = \sqrt{PGA_X PGA_Y} \tag{8}$$

In Eq. (6) through Eq. (8), accelerations are in g, PGA_X and PGA_Y are the PGAs of the horiztal components of ground motion in g, and PGA_V is the earthquake's vertical component PGA in g. Table 2 shows the performance of the PSDMs presented in Eq. (6) and Eq. (7), which indicates high accuracy of these models in predicting the cask's CG maximum accelerations.

Table 2 – Performance of the PSDMs developed for the maximum horizontal and vertical accelerations of the cask's center of gravity ($RMSE$: Root Mean Squared Error)

Model	5-Fold CV R^2	$RMSE$	p-Value					
			Intercept	μ	PGA_H	$\log PGA_H$	PGA_V	$\log PGA_V$
Eq. (6)	0.90	0.1447	---	2.7E-9	0.0001	6.7E-185	---	---
Eq. (7)	0.90	0.2256	1.3E-6	4.7E-7	---	2.4E-43	6.1E-7	9.5E-36

To develop the probabilistic demand model for the sliding response, the outputs of Eq. (6) and Eq. (7) for the maximum horizontal and vertical accelerations of the cask's CG, the geometric, material, and structural properties of the cask, the value of R_S, and the coefficient of friction between the cask and the pad were tested as predictors. Repeating the stepwise procedure, explained in this section, resulted in Eq. (9), where δ_{Max} is the maximum sliding of the cask in m.

$$\log \delta_{Max} = -2.794 \log D_C - 1.449 \log \mu + 3.707 \log a_{CG,H} - 0.172 R_S \tag{9}$$

$$R_S = \frac{\mu}{\frac{a_{CG,H}}{g - a_{CG,V}}} \tag{10}$$

The goodness of fit measurements showing the performance of this model are presented in Table 3. It should be mentioned that $a_{CG,H}$ and $a_{CG,V}$ predicted by Eq. (6) and Eq. (7), and not those resulting from the finite element analysis, were used as predictors as well as in calculating R_S, which means the error coming from Eq. (6) and Eq. (7) was propagated into the final PSDM for the sliding response. However, as Table 3 shows, Eq. (9) provides a relatively accurate prediction for the maximum sliding of the dry cask. Morover, the final model parameters are consistent with the physics of the problem. That is, the sliding distance reduces as the the coefficient of friction or R_S increases, and it increases with an increase in the horizontal acceleration of the cask's CG.

Table 3 – Performance of the PSDMs developed for the maximum sliding of the cask ($RMSE$: Root Mean Squared Error)

Model	5-Fold CV R^2	$RMSE$	p-Value			
			$\log D_C$	$\log \mu$	$\log a_{CG,H}$	R_S
Eq. (9)	0.91	0.5799	1.8E-57	2.5E-12	1.1E-86	0.0001

One of the applications of the models presented in this study is to estimate the maximum sliding of a cask given its outer diameter, the coefficient of friction, and the horizontal and vertical PGAs expected at the cask's site. As an example, for a cask with $D_C = 3.45$ m and $\mu = 0.5$ at a site with $PGA_H = 0.8\ g$ and $PGA_V = 0.5\ g$, Eq. (6) and Eq. (7) result in $a_{CG,H} = 0.922\ g$ and $a_{CG,V} = 0.978\ g$, respectively. Therefore, $R_S = 0.012$ and the maximum sliding response is estimated as $\delta_{Max} = 0.06$ m. It should be mentioned that the values resulting from the calculations are estimated responses, and not exact values. That is because each of the developed models follows a probability distribution, and the prediction of the model is the mean value of that distribution. In this study, Eq. (6), Eq. (7), and Eq. (9) assume normal distributions for the responses, which means $\log a_{CG,H}$, $\log a_{CG,V}$, and $\log \delta_{Max}$ follow normal distributions whose mean values are given by the equations. These normal distributions are used in the next section to develop fragility models for the sliding response, knowing that the standard deviations of the distributions are the $RMSE$ values given in Table 2 and Table 3 [18, 19].

The proposed method in this study is compared with the Reserve Energy approach in ASCE/SEI 43-05 [20] in which the effective coefficient of friction (μ_e) and sliding coefficient (c_S) are calculated as follows in Eq. (11) and Eq. (12), respectively.

$$\mu_e = \mu\left(1 - 0.4\frac{PGA_V}{g}\right) = 0.4 \tag{11}$$

$$c_S = 2\mu_e g = 7.848 \text{ m/s}^2 \tag{12}$$

Assuming 1D motion, using the 10% damped response spectral accelerations (SA_{VH}) used in ASCE/SEI 43-05 [20] and scaling it to $PGA_H = 0.8\,g$, the lowest frequency (f_{es}) at which $SA_{VH} = c_s$ is determined as $f_{es} =$ 1.99 Hz, which results in the best estimate for sliding (δ_S) in Eq. (13).

$$\delta_S = \frac{c_S}{(2\pi f_{es})^2} = 0.05 \text{ m} \tag{13}$$

The results for the maximum sliding distance, estimated by the PSDMs developed herein and ASCE/SEI 43-05 method in this example, are very close. However, the Reserve Energy method in ASCE/SEI 43-05 just reports the best estimate of the response and does not provide any probability distribution for that. Moreover, it needs more steps, including developing acceleration response spectrum. Therefore, the proposed method in this study is easier to use and can be applied in probabilistic studies to estimate large sliding responses as well.

4. Fragility estimation and sensitivity analysis

4.1 Fragility estimation for the sliding response

In its traditional form, a seismic fragility model offers the conditional probability of the response exceeding a specific capacity limit (e.g. the probability of the maximum sliding exceeding 0.1 m) given a measure of the seismic intensity. In this study, fragility surfaces were developed for the limit proposed by Singh et al. [5], $0.25D_C$, for the sliding response. Eq. (14) defines the mathematical relationship to determine the fragility.

$$P(\delta_{Max} > 0.25D_C|PGA_H, PGA_V) = \int_{a_{CG,H}=0}^{\infty}\int_{a_{CG,V}=0}^{\infty} P\left(\delta_{Max} > 0.25D_C\middle|a_{CG,H}, a_{CG,V}\right) f_{a_{CG,H},a_{CG,V}}\left(a_{CG,H}, a_{CG,V}\middle|PGA_H, PGA_V\right) da_{CG,V}\, da_{CG,H} \tag{14}$$

In this equation, $P\left(\delta_{Max} > 0.25D_C\middle|a_{CG,H}, a_{CG,V}\right)$ can be determined knowing that $\log \delta_{Max}$ is normally distributed with the mean value given by Eq. (9) and a standard deviation equal to the $RMSE$ value shown in Table 3. Moreover, $f_{a_{CG,H},a_{CG,V}}$ is the probability density function of the joint distribution of $\log a_{CG,H}$ and $\log a_{CG,V}$, which was assumed to have a bivariate normal distribution [21] with the mean values presented in Eq. (6) and Eq. (7) and standard deviations shown in Table 2 under the $RMSE$ column. The correlation coefficient of $\log a_{CG,H}$ and $\log a_{CG,V}$ was found to be 0.88. The resulting fragility surface for a cask with $D_C = 3.45$ m and $\mu = 0.5$ is illustrated in Fig. 4, and the corresponding probability contours are shown in Fig. 5. The results indicate that the fragility is mainly influenced by PGA_H. That is because PGA_H detemines $a_{CG,H}$ and $a_{CG,V}$ via Eq. (6) and Eq. (7), respectively, and as Eq. (9) shows, $a_{CG,H}$ directly affects the probability of failure. Therefore, larger values of PGA_H result in larger acclererations at the cask's center of gravity, and the larger accelerations cause larger sliding responses, which leads to higher probability of exceeding the sliding limit. In comparison, the influence of PGA_V on the fragility occurs through $a_{CG,V}$ and its impact on R_S value, and since the model parameter corresponding to R_S is relatively small in Eq. (14), the impact of PGA_V on the fragility is smaller. It should be mentioned that due to the lower effect of PGA_V on the fragility, the y-axis in Fig. 5 is in logarithmic scale.

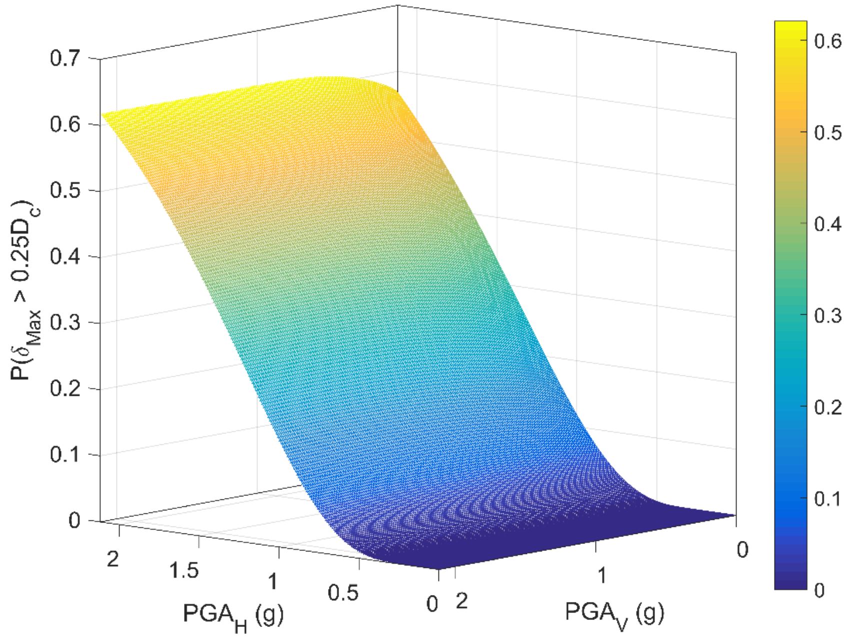

Fig. 4 – Fragility surface for the sliding response of a cask with $D_C = 3.45$ m and $\mu = 0.5$

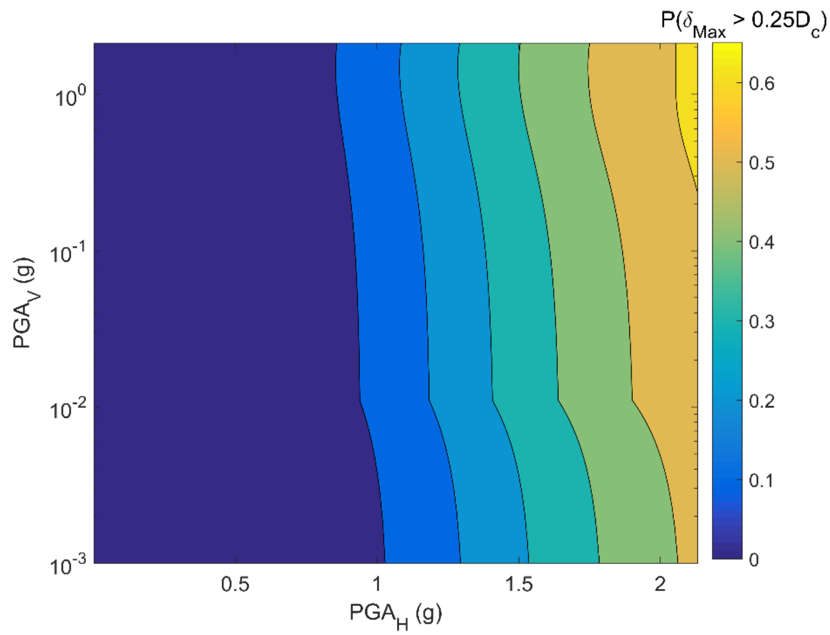

Fig. 5 – Probability contours corresponding to the fragility surface for the sliding response of a cask with $D_C = 3.45$ m and $\mu = 0.5$

4.2 Sensitivity analysis

As Eq. (9) shows, the maximum sliding response of a cask subject to an earthquake depends on the cask's outer diameter, the coefficient of friction between the cask and its support, the maximum horizontal acceleration of the cask's center of gravity, and the R_S value. In order to study the sensitivity of the fragility to the cask's diameter and the coefficient of friction, fragility curves were developed for scenarios with different values for D_C and μ. Since the sensitivity of 3D fragility surfaces is more challenging to interpret, only the cross sections of the fragility surface in which $PGA_V = 0.5\ g$ are shown in Fig. 6 as an example. As the figures show, the fragility is sensitive to the entire range of the cask's diameter, and the probability of failure decreases consistantly with increase in the diameter. Regarding the effect of the coefficient of friction on the fragility, illustrated in Fig. 6.b, the probability of failure is larger for $\mu = 0.2$, and it decreases as the coefficient of friction goes up to 0.35. The curves for other three values of coefficient of friction are very close to each other, however, which means increasing μ beyond 0.5 does not have a significant impact on the probability of faillure.

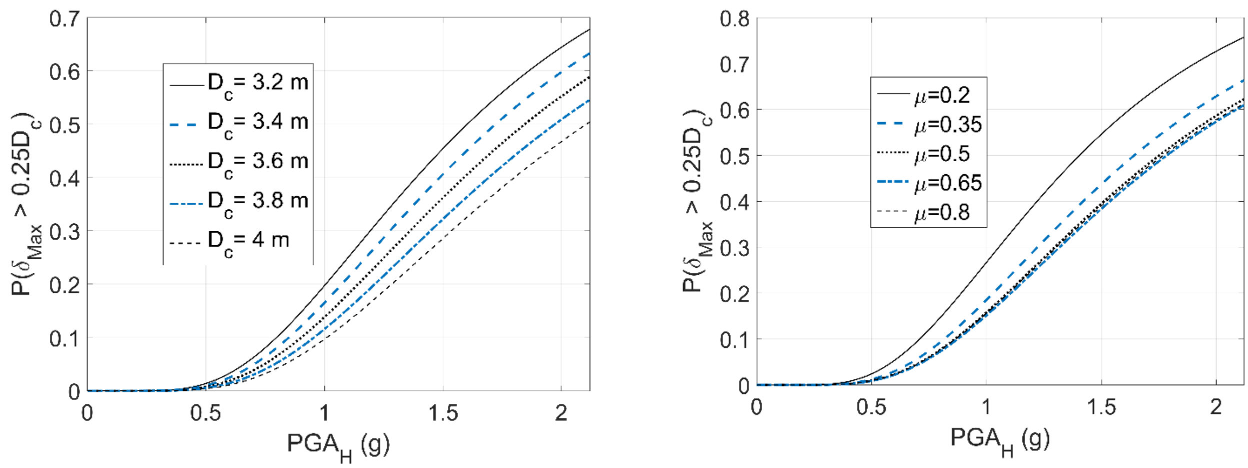

a b

Fig. 6 – Cross sections of the fragility surface for the sliding response at $PGA_V = 0.5\ g$ (a: $\mu = 0.5$, b: $D_C = 3.45$ m)

5. Conclusions

Nonlinear finite element models of the seismic response of dry cask structures were developed and verified in this study. Based on the literature, geometric, material, and structural parameters which might affect the seismic response were identified. 160 configurations, generated by the Latin hypercube sampling method, were paired with earthquake records representative of various regions across the U.S. with independent spent fuel storage installations. The generated finite element models were analyzed by LS-DYNA explicit solver, and the results were used to develop probabilistic seismic demand models for the sliding response using stepwise regression. The developed probabilistic demand models showed that the horizontal and vertical PGAs are suitable intensity measures of the seismic hazard to use as predictors of cask sliding. Moreover, maximum sliding of a cask subject to an earthquake depends on the outer diameter of the cask, the coefficient of friction between the cask and its support, the maximum horizontal acceleration of the cask's center of gravity, and R_S value ($R_S = \frac{\mu}{\frac{a_{CG,H}}{g-a_{CG,V}}}$). Using the proposed PSDM, a representative fragility surface was developed for the sliding response and the controlling limit proposed by Singh et al. ($0.25D_C$). The fragility analysis, performed in this study, could inform seismic rick estimates of the dry cask storage system at locations with appreciable seismic hazard levels. A sensitivity study was also conducted to illustrate how various significant parameters in the predictive model affect the final fragility estimate. Such sensitivity analyses on the fragility could help designers to have a better understanding of how changing the model variables affects the probability of failure.

6. Acknowledgements

The authors wish to acknowledge the support of the U.S. Department of Energy under the U.S. Department of Energy's Nuclear Energy University Program grant number 00128931 for this research project. The authors also acknowledge the Rice University Supercomputer Facility for providing computing resources used in conducting the research reported in this paper. The simulations were performed using the cyber infrastructure supported by NSF Grant OCI-0959097.

7. References

[1] Ko YY, Hsu SY, Chen CH (2009): Analysis for seismic response of dry storage facility for spent fuel. *Nuclear Engineering and Design*, **239**, 158-168.

[2] U.S. Nuclear Regulatory Commission (2007): A pilot probabilistic risk assessment of a dry cask storage system at a nuclear power plant. *NUREG-1864,* U.S. Nuclear Regulatory Commission, Washington, D.C., USA.

[3] Moore DP, Bjorkman GS, Kennedy RP (2000): Seismic analysis of plant hatch ISFSI pad and instability assessment of dry casks. *Proceedings of the 8th International Conference on Nuclear Engineering ICONE 8,* Baltimore, MD, USA.

[4] Bjorkman GS, Moore DP, Molin JJ, Thompson VJ (2001): Influence of the ISFSI design parameters on the seismic response of dry storage casks. *16th International Conference on Structural Mechanics on Reactor Technologu SMiRT 16,* Washington, D.C., USA.

[5] Singh KP, Soler AI, Smith M (2001): Predicting the structural response of free-standing spent fuel storage casks under seismic events. *16th International Conference on Structural Mechanics in Reactor Technology SMiRT 16,* Washington, D.C, USA.

[6] Shaukat SK, Luk VK (2002): Seismic behavior of spent fuel dry cask storage systems. *Proceedings of the 10th International Conference on Nuclear Engineering ICONE 10,* Arlington, VA, USA.

[7] Luk VK, Spencer BW, Shaukat SK, Lam IP, Dameron RA (2003): Sensitivity analyses of seismic behavior of spent fuel dry cask storage systems. *Proceedings of the 17th International Conference on Structural Mechanics in Reactor Technology SMiRT 17,* Czech Republic.

[8] U.S. Nuclear Regulatory Commission (2005): Parametric evaluation of seismic behavior of freestanding spent fuel dry cask storage systems. *NUREG/CR-6865, SAND2004-5794P*, U.S. Nuclear Regulatory Commission, Washington, D.C., USA.

[9] LS-DYNA (2012): Theory manual (version 971). Livermore Software and Technology Corporation.

[10] Shirai K, Hirata K, Saegusa T (2003): Experimental studies of free-standing spent fuel storage cask subjected to strong earthquakes. *17th International Conference on Structural Mechanics in Reactor Technology SMiRT 17,* Czech Republic.

[11] American Society of Civil Engineers (2000): Prestandard and commentary for the seismic rehabilitation of buildings. *FEMA 356,* American Society of Civil Engineers, Reston, VA, USA.

[12] NEHRP Consultant Joint Venture (2012): *Soil-Structure Interaction for Building Structures*. NIST GCR 12-917-21.

[13] Mckay MD, Beckman RJ, Conover WJ (1979): A comparison of three methods for selecting values of input variables in the analysis of output from a computer code. *Technometrics*, **22** (2), 239-245.

[14] Baker JW, Lin T, Shahi SK, Jayaram N (2011): New ground motion selection procedures and selected motions for the PEER transportation research program. *PEER Report 2011/03,* University of California, Berkeley, CA, USA.

[15] U.S. Nuclear Regulatory Commission (1987): Standard review plan for the review of safety analysis reports for nuclear power plants. *NUREG-0800.* U.S. Nuclear Regulatory Commission, Office of Nuclear Reactor Regulation.

[16] Collett D (2002): *Modeling Binary Data.* Chapman & Hall.

[17] Dobson AJ (1990): *An Introduction to Generalized Linear Models.* Chapman & Hall.

[18] McCullagh P, Nelder JA (1990): *Generalized Linear Models.* Chapman & Hall, 2nd edition.

[19] Mitchell T (1997): *Machine Learning.* McGraw-Hill.

[20] American Society of Civil Engineers and Structural Engineers Institute (2005): *Seismic Design Criteria for Structures, Systems, and Components in Nuclear Facilities (ASCE/SEI 43-05).* VA, USA.

[21] Melchers RE (2002): *Structural Reliability Analysis and Prediction.* John Wiley & Sons, 2nd edition.